



## OPEN Hyoid bone-based sex discrimination among Egyptians using a multidetector computed tomography: discriminant function analysis, meta-analysis, and artificial intelligence-assisted study

Afaf Abdelkader<sup>1✉</sup>, Susan A. Ali<sup>2</sup>, Ahmed Abdeen<sup>3✉</sup>, Ehab S. Taher<sup>4</sup>, Asmaa Y. A. Hussein<sup>1</sup>, Mamdouh Eldesoqui<sup>5</sup>, Mohamed Abdo<sup>6,7</sup>, Liana Fericean<sup>8</sup>, Bănăţean-Dunea Ioan<sup>8✉</sup>, Samah F. Ibrahim<sup>9</sup>, Ashraf M. Said<sup>10</sup>, Darine Amin<sup>11</sup>, Elturabi E. Ebrahim<sup>12</sup>, Amany M. Allam<sup>13,14</sup>, Mihaela Ostan<sup>15</sup>, Khaled A. Bayoumi<sup>16,17</sup>, Tabinda Hasan<sup>18</sup> & Ekramy M. Elmorsy<sup>19,20</sup>

The hyoid bone has been identified as sexually dimorphic in various populations. The current study is a forerunner analysis that used three-dimensional multidetector computed tomography (3D MDCT) images of the hyoid bone to examine sexual dimorphism in the Egyptian population. A total of 300 subjects underwent neck CT imaging, with an additional 60 subjects randomly selected for model validation. Ten hyoid variables were measured. Initially, the dataset was subjected to discriminant analysis to predict sex and the critical variables associated with sexual dimorphism. Subsequently, machine learning approaches were employed to enhance the accuracy of sex determination. The results indicated that all measured dimensions of the hyoid bone were substantially larger in males confront to females. Discriminant functions combining four measurements (major and minor axes of the hyoid body, the distance between the lesser horns, and hyoid bone length) achieved a higher accuracy of sex prediction compared to univariate functions. The accuracies of machine learning models ranged from 0.8667 to 0.933 with precision, recall, and F1-scores also showing improvements. These findings underscore the robustness and reliability of hyoid bone in sex discrimination among Egyptians, supported by both traditional statistical methods and machine learning approaches, and could prove invaluable in forensic cases.

**Keywords** Egyptian population, Forensic anthropology, Sex discrimination, Hyoid bone, Meta-analysis, Multidetector computed tomography

### Abbreviations

AA'	Major axis of hyoid body
BB'	Minor axis of hyoid body
CC'	Thickness of hyoid body
Chi <sup>2</sup>	Chi-square
Cis	Confidence intervals
DD'	Length of right greater horn
D'E'	Distance between the posterior end of greater horns
DFA	Discriminant function analysis
EE'	Length of left greater horn
FF'	Distance between the lesser horns
GG'	Distance between the centers of greater horns
HL	Hyoid bone length

HW	Hyoid bone width
I <sup>2</sup>	Inconsistency
MDCT	Multidetector computed tomography
NPV	Negative predictive value
PCA	Principal component analysis
PPV	Positive predictive value
Tau <sup>2</sup>	Tau-square
3D CT	Three-dimensional computed tomography

<sup>1</sup>Department of Forensic Medicine and Clinical Toxicology, Faculty of Medicine, Benha University, Benha 13518, Egypt. <sup>2</sup>Department of Radiodiagnosis, Faculty of Medicine, Ain Shams University, Cairo 11591, Egypt. <sup>3</sup>Department of Forensic Medicine and Toxicology, Faculty of Veterinary Medicine, Benha University, Toukh 13736, Egypt. <sup>4</sup>Department of Basic and Clinical Medical Sciences, Faculty of Dentistry, Zarqa University, Zarqa 13110, Jordan. <sup>5</sup>Department of Basic Medical Sciences, College of Medicine, Almaarefa University, P.O. Box 71666, Riyadh 11597, Saudi Arabia. <sup>6</sup>Department of Animal Histology and Anatomy, School of Veterinary Medicine, Badr University in Cairo (BUC), Badr City 32897, Egypt. <sup>7</sup>Department of Anatomy and Embryology, Faculty of Veterinary Medicine, University of Sadat City, Sadat City, Egypt. <sup>8</sup>Department of Biology and Plant Protection, Faculty of Agriculture, University of Life Sciences "King Michael I" from Timișoara, Calea Aradului 119, CUI 3487181 Timisoara, Romania. <sup>9</sup>Department of Internal Medicine, College of Medicine, Princess Nourah bint Abdulrahman University, P.O. Box 84428, Riyadh 11671, Saudi Arabia. <sup>10</sup>Biomedical Engineering Program, Department of Electrical Engineering, Benha University, Benha 13518, Egypt. <sup>11</sup>Department of Biological Anthropology, Medical Research and Clinical Studies Institute, National Research Center, Giza 12622, Egypt. <sup>12</sup>Department of Medical-Surgical Nursing, College of Nursing, Prince Sattam bin Abdulaziz University, Al-Kharj 11942, Saudi Arabia. <sup>13</sup>Department of Anatomy and Embryology, Faculty of Medicine, Benha University, Benha 13518, Egypt. <sup>14</sup>Department of Anatomy, Physiology, and Biochemistry, Faculty of Medicine, The Hashemite University, P.O. Box 330127, Zarqa 13133, Jordan. <sup>15</sup>Department of Biology, University of Life Sciences "King Michael I" from Timișoara, Calea Aradului, Timisoara, Romania. <sup>16</sup>Department of Pathology, Faculty of Medicine, King Abdulaziz University, Jeddah, Saudi Arabia. <sup>17</sup>Department of Forensic Medicine and Clinical Toxicology, Faculty of Medicine, Cairo University, Cairo 12613, Egypt. <sup>18</sup>Department of Anatomy, College of Medicine, Princess Nourah bint Abdulrahman University, P.O. Box 84428, Riyadh 11671, Saudi Arabia. <sup>19</sup>Center for Health Research, Northern Border University, Arar 91431, Saudi Arabia. <sup>20</sup>Department of Forensic Medicine and Clinical Toxicology, Faculty of Medicine, Mansoura University, Mansoura 35516, Egypt. ✉email: afaf.abdelkader@fmed.bu.edu.eg; ahmed.abdeen@fvmt.bu.edu.eg; ioan\_banatean@usvt.ro

The ascertainment of anonymized individuals is a pivotal issue in the field of forensic medicine. It can direct the medicolegal interrogator to the real identity of a decedent amongst a wide assortment of potential counterparts<sup>1</sup>. In particular, the challenging crime inquiry that is needed in sophisticated cases such as mass disasters, investigation of dismembered, robustly decomposed, or badly mutilated corpses, or skeletal remnants that are difficult to identify by fingerprint matching<sup>2</sup>. It is well known that sex discrimination is a principal step in any forensic investigation since it serves as a base for evaluating other biological features including racial descent<sup>3,4</sup>. When compared to other complicated tissue identification procedures, sex discrimination by means of skeletal remains has proven to be a helpful and trustworthy method<sup>5</sup>. Notwithstanding the skull and pelvis are the fundamental bones in sex identification, although substitutional methods based on other bones are encouraged in case they are missing<sup>2,4,6</sup>.

Hyoid bone is a distinctive short bone present in the middle of the anterior aspect of the neck and lies approximately at the level of the third cervical vertebra<sup>7,8</sup>. A vastly increased body of literature strongly implied that the hyoid bone has sexually dimorphic traits<sup>2,9,10</sup> and consequently, it has a legal significance in sex determination depending on both morphological features and metric measurement<sup>10–13</sup>. Nevertheless, the morphological approaches that rely on visual scrutiny of sexual distinction, do not appear to be adequate tools in forensic practice<sup>9</sup>. Conversely, the computational metric techniques are outshined in sexual discrimination due to their easy applicability and high precision without the interference of human error<sup>14</sup>. Among these, multidetector computed tomography (MDCT) has shown enhanced precision of sex determination through hyoid measuring compared to other techniques as it grants envisage nearly every anatomical structure with superb resolution and quality. As a consequence, 3D CT images may be efficiently used to delineate criteria for the evaluation of biological features in the skeleton<sup>2</sup>.

Furthermore, a newly emerging machine learning-based approach, a subset of artificial intelligence, is widely used lately in a bio-archaeological investigation of sex estimation. These techniques can be applied individually or in conjunction with more conventional statistical techniques to offer predictions obtained from metric methods based on strong mathematical concepts<sup>15</sup>. Prior research on anthropometric measures of various bones has demonstrated higher rates of sexual dimorphism by using discriminant function analysis (DFA) as well as machine learning techniques<sup>16</sup>.

Furthermore, ample research has highlighted that besides individual variances, population differences influence the traits that determine the sex<sup>17</sup>. Therefore, to optimize the precision of sex determination, unique methods ought to be developed for creating predictive equations for hyoid sexing in humans which is region and population-specific<sup>2,9,10,12</sup>.

To date, sundry studies have investigated the sexual dimorphism of the hyoid bone, either utilizing only conventional statistical methods or discriminate function analysis. To the best of our knowledge, a literature survey finds that, no data evaluating the outcomes of hyoid bone measurements using a machine learning approach among Egyptians. In line with this assertiveness, the current study examines the accuracy of sex estimation using various machine learning classifiers and model selection techniques, as a novel approach

in hyoid bone sexual dimorphism, in addition to discriminate function analysis, using measurements from reformatted images of 3D MDCT of hyoid bone in contemporary Egyptian population. Moreover, we have performed a meta-analysis to test whether hyoid measurements used in our study are efficient predictors of sex comparable to other related reports carried out among different populations.

Materials and methods

Dataset

A total of 300 randomly chosen adult Egyptians of known age (18–85 years old) and sex (150 male and 150 female) were subjected to high-resolution 3D MDCT neck scans at the CT Unit, Department of Radiodiagnosis, Ain Shams University Hospital, Egypt, for reasons other than neck pathologies were included (Group-I). The preadolescents’ bones are practically worthless for determining sex because the secondary sexual traits don’t develop till the remodeling of bones under the effects of estrogen and androgen at puberty<sup>18</sup>. Hence, samples under the age of 18 were not included in our investigation. In addition, another 60 samples (30 females and 30 males) were used to validate the prediction model set from the first group data (Group-II).

Exclusion criteria: cases with hyoid bone fractures, neck injuries, any pathological lesions, likewise bone dysplasia, metabolic bone diseases, connective tissue disorders or arthritis, prior orthopedic surgery as well, and bone tumors were excluded to ensure normal bone evaluation.

The obtained data were analyzed under rigorous anonymity. The procedures were authorized by the Ethical Committee of Faculty of Medicine, Ain Shams University (FMASU R 09/2019). The Declaration of Helsinki, the International Medical Association’s code of ethics, was followed in this study.

Multidetector computed tomography (MDCT) protocol of image acquisition

MDCT neck scanning was done using a 128-row detector CT system, a 128 multi-slice CT scanner (Optima 660, GE, USA) without contrast material. Patients were imaged in a supine position and the scanning protocol was as follows image parameters: slice thickness of 2.5 mm, collimation of 0.625 mm, reconstruction interval of 0.625 mm, tube voltage of 120 kVp, tube current of 200 mAs, and rotation time of 1 per second. To prevent technical variances in length and volume measurements, the scan acquisition technique was the same for every patient.

Reconstruction and post-processing

Image data were processed on a workstation (AW Volume Share 7, GE, France) for the reconstruction of high-quality 3D models using the volume rendering technique. The 3D images of the hyoid bone were prepared first, checked for tilt, and corrected to ensure that when viewed, it was oriented correctly. The Advantage Workstation’s measuring tool software was used to measure the distances between each part of the hyoid bone at a 13 cm field of view.

Measurements on the hyoid bone 3D-CT images

Ten variables were investigated for each hyoid bone employing electronic cursors to the closest 0.1 mm in accordance with previous studies protocols<sup>2,19</sup> (Table 1; Fig. 1).

To evaluate intra-observer error, the radiology specialist collected the subset data in two sessions, and another coauthor (forensic doctor) gathered the subset data to evaluate inter-observer error. A subset of 20 subjects (10 males and 10 females) were selected at random. Thereafter, the technical error of measurements, relative technical error of measurements (rTEM, %), and coefficient of reliability (R) were calculated. The acceptance ranges of rTEM for intra-observer errors and inter-observer errors were <1.5 and <2.0%, respectively; the R-value, which demonstrates the proportion of the between-subject variance free of measurement errors, of >0.75 was considered sufficiently precise<sup>2,20</sup>.

Dimension	Description
AA’	Major axis of hyoid body (Hyoid body width)
BB’	Minor axis of hyoid body (Hyoid body length)
CC’	Thickness of hyoid body (Anteroposterior length)
DD’	Length of right greater horn
EE’	Length of left greater horn
FF’	Distance between the lesser horns
GG’	Distance between the centers of greater horns
D’E’	Distance between the posterior end of greater horns
HW	Hyoid bone width (Linear distance between the most lateral points of the greater horns of the hyoid bone)
HL	Hyoid bone length (Perpendicular length from the most anterior edge of the hyoid body to the line that connects the most distal points of the greater horns of the hyoid bone)

Table 1. Description of measurements used for hyoid bones.

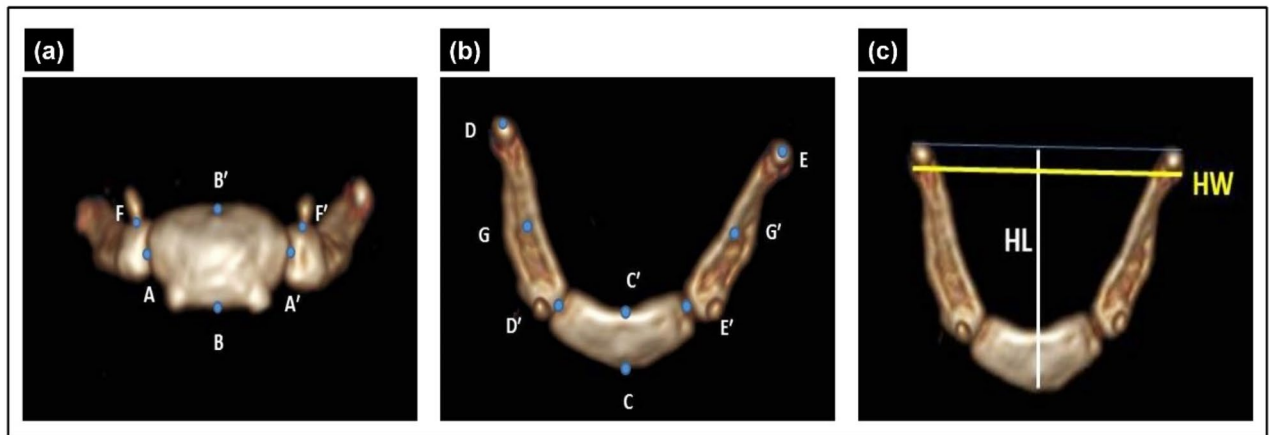


**Fig. 1.** 3D images of hyoid bone illustrating the different measurements. (A) Showed the major (AA') and minor (BB') axes of the hyoid body as well as the distance between the lesser horns (FF'). (B) Showed hyoid body thickness (CC'), right greater horn length (DD'), left greater horn length (EE'), the distance between the centers of greater horns (GG'), and the posterior distance between the greater horns (D'E'). (C) Showed the hyoid length (HL) and width (HW).

## Statistical analyses

### *Discriminant function analysis (DFA)*

Univariate and multivariate analyses were implemented using RStudio (Version RStudio 2022.12.0+353 “Elsbeth Geranium” Release (7d165dcfc1b6d300eb247738db2c7076234f6ef0, 2022-12-03) for Windows) and SPSS software (Version 21.00; SPSS Inc., Chicago, IL, United States). “Factoextra”, “FactoMineR”, “ggbetweenstats”, “ggpubr”, “ggplot2”, “ggstatsplot”, “ggExtra”, “hrbrthemes”, “easyGgplot2”, and “vcd” packages were installed in the RStudio for required data analyses and visualization. The values of each measured parameter were examined using the F-test for proportional variance in the mean values of females and males in order to assess the statistical relevance of sex disparities. When the variance was equal, the Student’s t-test was used, and Welch’s t-test was chosen for the unequal variance at the statistical significance level of  $p$  0.05.

For each measurement of the hyoid bones, univariate discriminant function models for sex categorization were developed to get demarcating points for males and females which might be applied to fragmented bones. In addition, stepwise DFA was implemented to all dimensions, utilizing Wilks’  $\lambda$  minimization, in order to identify which combination of variables provided the best discrimination between the sexes. Functions at group centroids were computed, and they represent the means of the discriminant function scores by group for each function. The eigenvalue was measured to evaluate how well that function differentiates between the groups, where the higher the eigenvalue, the better the function differentiation. The higher the canonical correlation and the proximity of the eigenvalue to 1, the higher the discrimination accuracy was. Additionally, Wilks’  $\lambda$  was determined to assess how well each level of independent variable isolated subjects into male and female sets; with values near to 0 indicating total discrimination and values near to 1 indicating no discrimination. The equations with higher percentages of precise sex classification were selected. Using the leave-one-out cross-validation method, accurate classification rates of derived discriminant function equations were computed. An additional validation of our model was performed with testing data (validation sets) consisting of 60 samples (30 females and 30 males). The accuracy of the discriminate function was evaluated using the ROC curve.

### *Meta-analysis*

A meta-analysis was conducted to integrate comparable outcomes in each category by using RevMan (version 5.0, Copenhagen: Nordic Cochrane Centre, Cochrane Collaboration, 2008). The included studies (Inclusion criteria) introduce comparisons between males and females for two or more hyoid bone measurements (major axis, minor axis of the hyoid body, distance between lesser horns, and length of hyoid bone). Only studies written in the English language published in international publications and had enough information for qualitative and quantitative analyses were included. The studies did not suggest sufficient data or introduce measurements for one arm only males or females were excluded. Also, animal research, posters, duplicate papers, or conference papers were not included (Fig. 2).

The following terms were used for the search strategy (Forensic anthropology, Multidetector computed tomography, Hyoid bone, Egyptian, Sex estimation). We exported the searched studies to EndNote X9.1 (Clarivate Analytics, <https://clarivate.com/>) to remove duplicates. Two independent reviewers screened all records for eligibility. Eligibility screening was performed in two steps: in the first step, titles and abstracts were screened, and in the second step, full-text articles of the selected abstracts were retrieved and assessed for eligibility. Disagreements were resolved by discussion with a third reviewer. Laboratory values, treatments, and results were extracted. Two independent reviewers extracted data to a uniform Microsoft Excel sheet. To ensure

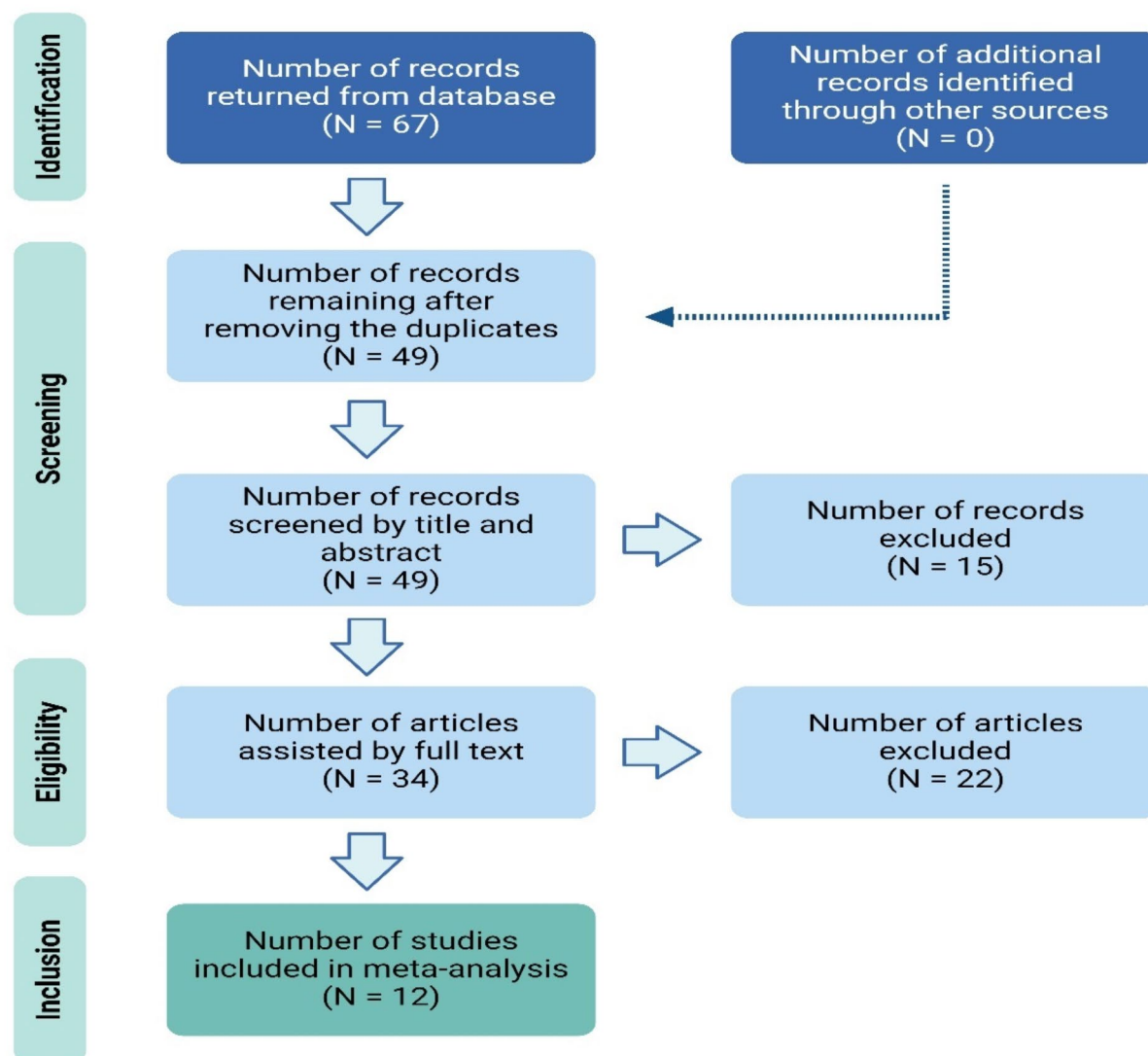


**Fig. 2.** Meta-analysis flowchart. Flow diagram demonstrating study selection for meta-analysis.

data accuracy, a third independent reviewer conducted an additional check on the data that was retrieved. All disagreements were resolved through discussion.

To test for heterogeneity, the inconsistency ( $I^2$ ), Chi-square ( $\chi^2$ ), and Tau-square ( $\tau^2$ ) tests were employed. Results with less heterogeneity ( $I^2 < 50\%$ ) were presented with a random-effects model and sensitivity analysis was conducted to show the power of effect estimate when leave-out-one study in each scenario. Forest plots were created from continuous data using weighted mean differences. Heterogeneity was determined among the included studies by visual checking of the forest plots to identify the pooled estimates' 95% confidence intervals (CIs).  $I^2$  values of 25%, 50%, and 75%, might be classified as low, moderate, and high heterogeneity, respectively, according to Higgins et al.<sup>21</sup>. Inverse variance statistical analysis was used to evaluate the results. Negative values represent a decrease, whereas positive percentage changes indicate an increase in the relevant variables. Moreover, 95% CIs and mean effect sizes were calculated by applying Meta Win 2.0's bootstrapping process, which included 4999 iterations. If the 95% CIs of the categorical variables did not overlap, then the means of the variables were significantly different from one another.

#### *Machine learning approach (prediction algorithms)*

In our investigation into the discriminatory potential of hyoid bone measurements for sex prediction, we utilized a multi-faceted machine learning approach. Following the initial data preprocessing phase, where measurements from 300 subjects were prepared for analysis, we embarked on a rigorous feature selection process. Employing lasso regression, we identified the most predictive feature, labeled "AA", for sex prediction.



Subsequent to feature selection, we explored a variety of machine learning algorithms, each chosen for its unique approach to classification according to Attia and Said<sup>22</sup>:

1. Gradient boosting classifier: we applied an ensemble technique that combines multiple weak prediction models, primarily decision trees, to form a strong predictor. The iterative correction of errors by new trees is mathematically represented as  $F_m(x) = F_{m-1}(x) + \rho_m h_m(x)$ , where  $F_{m-1}(x)$  denotes the model from the previous iteration,  $h_m(x)$  signifies the weak learner added at iteration  $m$ , and  $\rho_m$  is the learning rate.
2. Random forest classifier: this algorithm uses an ensemble of Decision Trees, trained with the “bagging” method, to make predictions by averaging the outcomes of  $N$  individual trees:

$$y(x) = \frac{1}{N} \sum_{i=1}^N t_i(x).$$

3. K-nearest neighbors (KNN) classifier: the KNN algorithm predicts the output based on a majority vote from the  $k$  closest training examples in the feature space:  $y(x) = \frac{1}{k} \sum_{i \in N_k(x)} y_i$ .
4. Gaussian Naïve Bayes (GNB) classifier: applying Bayes' theorem with the assumption of independence among features, the class probability is given by  $P(y|x_1, \dots, x_n) = \frac{P(y) \prod_{i=1}^n P(x_i|y)}{P(x_1, \dots, x_n)}$ .
5. Support vector machine (SVM) classifier: we sought a hyperplane that best separates the classes by maximizing the margin between the closest points of the classes, described mathematically as  $f(x) = \text{sgn}(w^T x + b)$ .
6. Decision tree classifier: this model utilizes feature value tests to split data into subsets, aiming for maximum purity in each subset, with decisions based on maximizing information gain  $IG$ .
7. Logistic regression classifier: employing a logistic function to estimate probabilities, the model  $\sigma(z) = \frac{1}{1+e^{-z}}$ , where  $z = w^T x + b$ .
8. Voting classifier: an ensemble meta-model that combines predictions from the aforementioned classifiers, utilizing either ‘hard’ or ‘soft’ voting strategies to finalize the prediction. The output label is the prediction with the highest average probability of all the individual classifiers. The decision function can be represented as:  $y(x) = \text{mode}(\{h_1(x), h_2(x), \dots, h_n(x)\})$ , where  $h_i(x)$  is the prediction of the  $i$ th classifier.

To optimize each model's performance, hyperparameter tuning was conducted using grid search, exploring various combinations to identify optimal settings. The performance of each algorithm was then evaluated using standard classification metrics, including accuracy, precision, recall, and F1-score, complemented by cross-validation to ensure robustness and generalizability.

After fine-tuning, models were reassessed to pinpoint the most effective based on performance metrics. The comprehensive analysis and interpretation of these machine learning models, alongside traditional statistical methods, provided a robust assessment of hyoid bone measurements' utility in sex prediction. This methodological approach underscores the innovative integration of advanced analytical techniques in medical research, offering insights into the potential of machine learning in enhancing diagnostic accuracy.

## Results

### Hyoid bone measurement values and sex differences

The rTEMs for intra-observer and inter-observer errors ranged from 0.446 to 1.292% and from 0.672 to 1.859%, respectively. The R values ranged from 0.963 to 0.999. The intra- and inter-observer reproducibility was very good for all measurements.

Ten dimensions of hyoid bone were measured as depicted in Figs. 3 and 4; mostly related to the lesser horns and the right and left greater horns and hyoid bodies. Out of these 10 measurements, 4 dimensions were related to hyoid horns and 3 were related to hyoid body measurements. Interestingly, significant disparities between males and females were observed in all measured dimensions; where males had greater hyoid bone measurements than females ( $p < 0.05$ ) and subsequently larger hyoid demonstrating the existence of substantial sexual dimorphism in hyoid measurements among Egyptian people.

As exhibited in Fig. 3A and B, the mean major axis and minor axes of the hyoid body were greater in males (24.3 and 11.32, respectively) than in females (19.8 mm and 9.85 mm, respectively). In addition, the mean thickness, mean width, and mean length of the hyoid bone in males and females (6.99 mm vs. 5.80 mm; 42.85 mm vs. 38.29 mm; 35.38 mm vs. 29.24 mm, respectively), as shown in Fig. 3C–E.

Furthermore, the mean lengths of the right and left greater horns of hyoid bones were larger in males (Rt = 27.63 mm and Lt = 27.0 mm) than in females (Rt = 23.39 mm and Lt = 23.17 mm), Fig. 4A and B, respectively. Figure 4C–E expound the distance between the greater horn centers, greater horn posterior ends, and distance between the lesser horns, which were greater in males (39.65, 35.32, and 26.33 mm, respectively) than in females (35.44, 30.51, and 22.35 mm, respectively). An example of different measurements of hyoid bone from our patients (35-year-old female and male) is represented in Fig. 5.

### Discriminant function equations (age prediction models and validation)

Discriminant function equations were created using the ten variables as predictors of sex. Table 2 displays the data of the univariate and stepwise DFA for the measurements of the hyoid bone.

According to univariate DFA, AA' showed the highest distinction ability of the discriminant, with a canonical correlation of 0.707; eigenvalue was 1.002, and Wilk's  $\lambda$  of a canonical discriminant function was 0.499, meaning

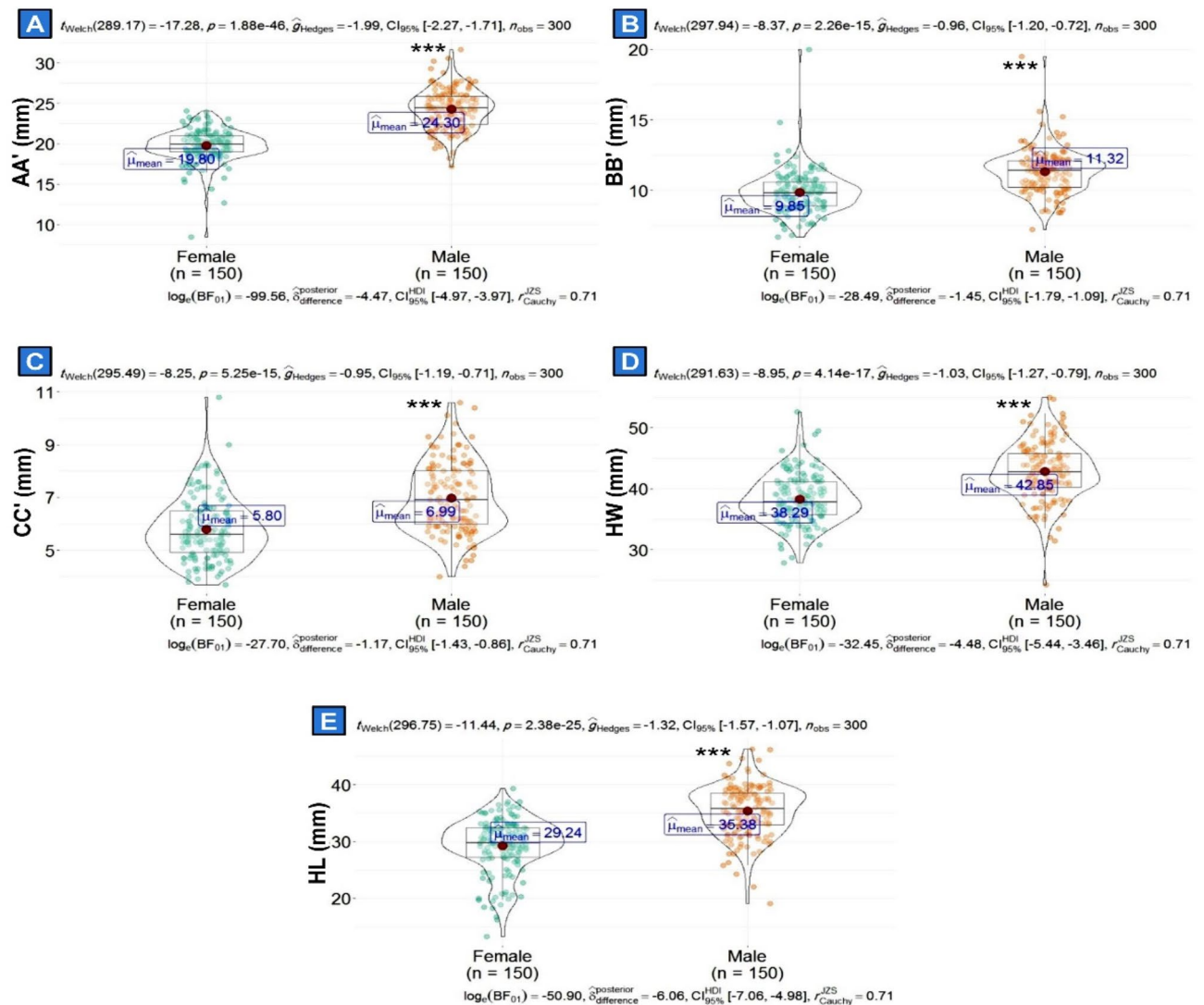


**Fig. 3.** Vilon-dot-plots of different lengths of hyoid bone in male and female patients. (A–E) Length of all tested bone types, including AA', BB', CC', HW, and HL, respectively. Asterisks indicate significant differences at  $P < 0.05$  based on Welch test. Total number of observations in males and females and the confidence interval are shown.

that there was a statistically meaningful discriminant score discrepancy among groups. Stepwise DFA using the combined 4 metric measurements (AA', BB', FF', and HL), yielded substantial statistical discriminant score variations between males and females, with a canonical correlation was 0.771 and the eigenvalue was 1.464. Wilk's  $\lambda$  of a discriminant function was 0.406 with  $P < 0.001$ .

The correct estimation rates of univariate discriminant analysis varied from 65.7 to 85%; the classification accuracy for males and females ranged from 60.7 to 80% and from 66 to 90%, respectively. When assessing single variables, the AA' dimension exhibited the highest over-accuracy rate (85%) (contributed most significantly to sex estimation), while the CC' measurement had the lowest accuracy rate (65.7%). The Cross-validated results of stepwise analyses provided more accurate classification rates than the univariate functions, with 87.7% of the cases accurately classified by the four-variable model.

Sixty hyoid samples were used as a validation set for the final prediction equation (Group 2). The predicted sex was calculated as  $\text{predicted sex} = 0.236(\text{AA}') + 0.167(\text{BB}') + 0.158(\text{FF}') + 0.077(\text{HL}) - 13.310$ . ROC curve analysis was then conducted to detect the diagnostic usefulness of the discrimination function for the estimation of sex. Table 3 shows the validity profile, the function, the cutoff point, overall accuracy, sensitivity, specificity, and positive and negative predictive values. A measured value above the demarking point (cutoff point,  $-0.4866$ ) classifies an individual as male as 87.5% of them were truly males (PPV), and a lower value point out to the female as 92.9% of them were truly females (NPV).

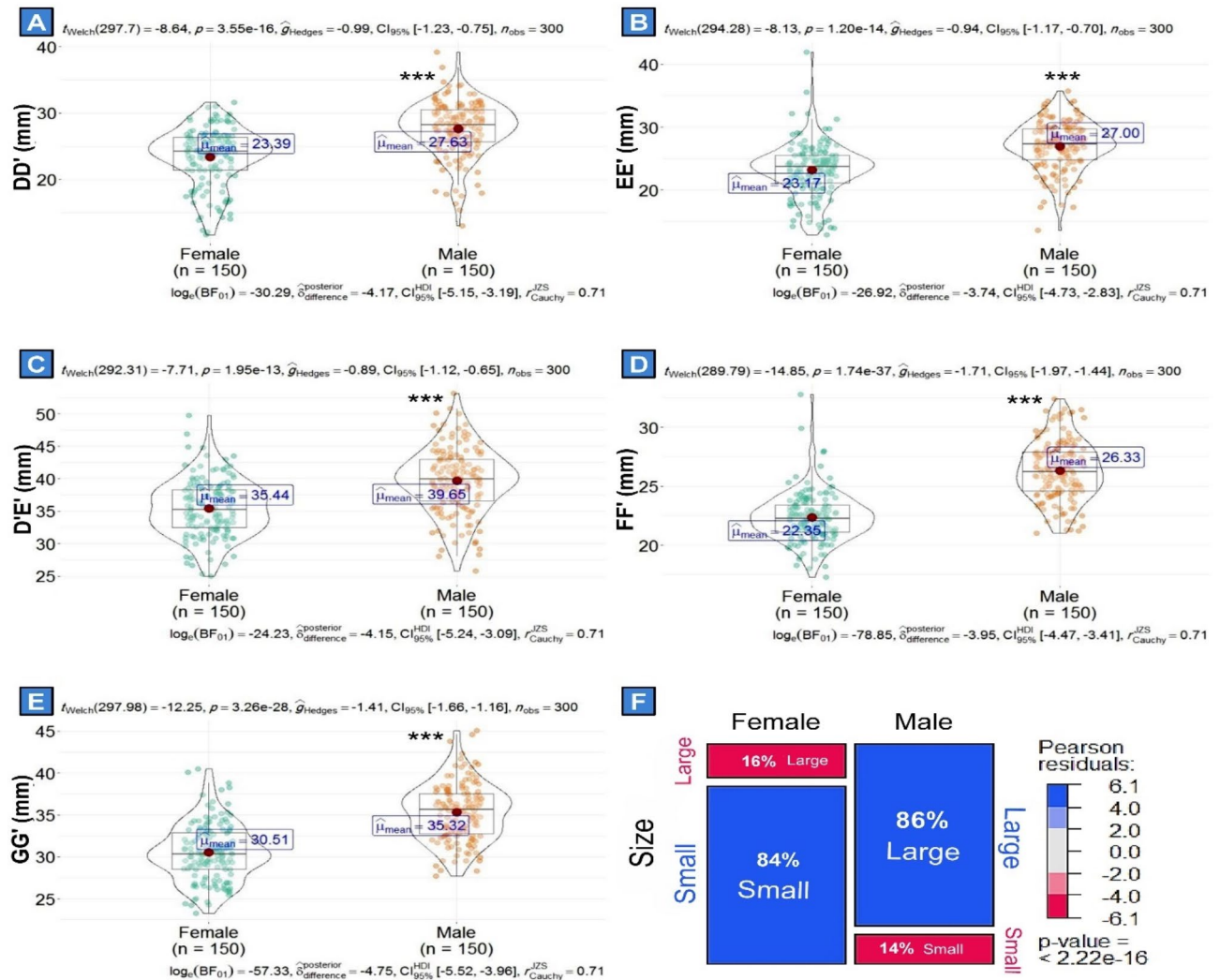


**Fig. 4.** Vilon-dot-plots of hyoid bone length in male and female patients. (A–E) Length of all tested bone types, including DD', EE', FF', GG', and D'E', respectively. Asterisks indicate significant differences at  $P < 0.05$  based on Welch test. Total number of observations in males and females and the confidence interval are shown. (F) Mosaic plot of proportional size differences of hyoid bone in male and female patients.

Data revealed that the AA', BB', FF', and HL dimensions were the best variables that can be used all together in proper sex estimation with a percentage of accuracies ranging between 79.49 – 96.24%. The discrimination function score can significantly predict sex. Table 4 shows a statistically insignificant relation between actual sex and predicted sex ( $P = 0.688$ ).

### Multivariate analyses

The Principal component analysis (PCA) score plot showed that the males were grouped together on the left side and separated from the females. As shown in Fig. 6A, PC1 differentiated most males, resulting in a higher percentage of variance (47.8%), whereas PC2 reported a lower percentage of variation (15.2%). All the studied parameters were incorporated into 3 principal components based on the 3D plot (PC1, PC2, and PC3), accounting for 72.2% of all variances. The majority of the tested parameters were distinct by PC1 and hence depicted by the largest proportion of variance (47.8%), whereas the smaller proportion of variation was distributed across PC2 (15.2%) and PC3 (9.2%), as shown in Fig. 6B. Loading plot PCA, revealed that AA', BB', FF', GG', HL, and HW dimension were the most contributed variables in the current study important in discrimination between male and female (most sexually dimorphic measurement) (Fig. 6C).

Alongside, the hierarchical clustering heatmap of the measured dimensions of hyoid bone in male and female patients expounded in Fig. 7 provides an axiomatic depiction of the entire data sets, which epitomizes the significant variation between the mean values of all measured variables in both sexes. These findings demonstrate how the males experienced larger dimensions than the females.



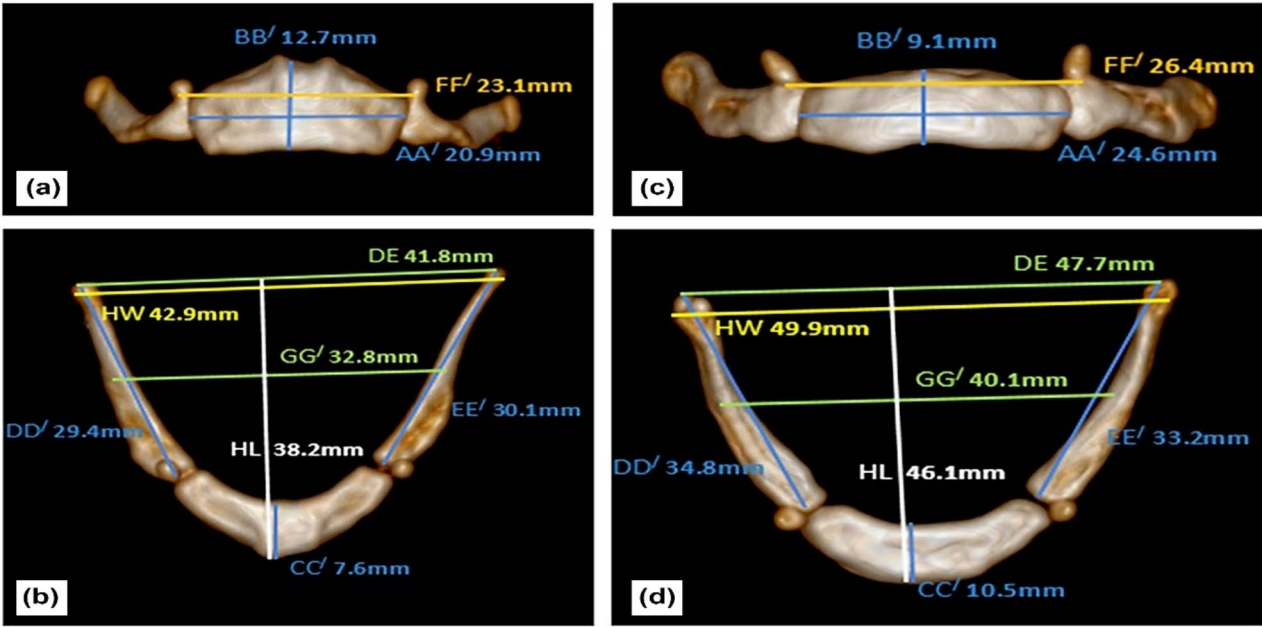


**Fig. 5.** 3D images illustrating the different measurements of hyoid bone. A 35 years old (A,B) female and male (C,D).

Equation	Group centroid		Eigenvalue	Wilks' $\lambda$	Canonical correlation	Total function accuracy		Accuracy of sexes			
	Male	Female				N	%	Male		Female	
								N	%	N	%
Univariate analysis											
0.443(AA') – 9.775	0.998	– 0.998	1.002	0.499	0.707	255	85	120	80	135	90
0.656(BB') – 6.943	0.483	– 0.483	0.235	0.810	0.436	215	71.7	104	69	111	74
0.803(CC') – 5.132	0.476	– 0.476	0.228	0.814	0.431	197	65.7	91	60.7	106	70.7
0.235(DD') – 6.006	0.499	– 0.499	0.250	0.800	0.447	212	70.7	113	75.3	99	66
0.245(E'E') – 6.155	0.469	– 0.469	0.222	0.818	0.426	218	72.7	110	73.3	108	72
0.430(FF') – 10.474	0.857	– 0.857	0.740	0.575	0.652	248	82.7	117	78	131	87.3
0.294(GG') – 9.689	0.707	– 0.707	0.503	0.665	0.579	225	75	111	74	114	76
0.211(D'E') – 7.928	0.445	– 0.445	0.200	0.834	0.408	207	69	105	70	102	68
0.215(HL) – 6.952	0.662	– 0.662	0.439	0.695	0.552	226	75.3	115	76.7	111	74
0.227(HW) – 9.192	0.517	– 0.517	0.269	0.788	0.460	217	72.3	110	73.3	107	71.3
Stepwise analysis											
0.236(AA') + 0.167(BB') + 0.158(FF') + 0.077(HL) – 13.310	1.206	– 1.206	1.464	0.406	0.771	263	87.7	128	85.3	135	90

**Table 2.** Univariate and stepwise discriminant function analysis for hyoid bones.

Function	Cutoff point	Significance (P)	AUC	Accuracy%	Accuracy of males (PPV, %)	Accuracy of females (NPV, %)
0.236 (AA') + 0.167 (BB') + 0.158 (FF') + 0.077(HL) – 13.310	– 0.4866	0.000	0.953	90% (79.49–96.24%)	87.50% (73.66–94.60%)	92.86% (77.18–98.04%)

**Table 3.** Validation of discriminant function for determining sex from hyoids using ROC curve. AUC area under the curve, PPV positive predictive value, NPV negative predictive value.

	Actual sex						P value
	Male		Female		Total		
	N	%	N	%	N	%	
Predicted sex							
Male	28	93.3	4	13.3	32	53.3	0.688
Female	2	6.7	26	86.7	28	46.7	
Total	30	100	30	100	60	100	

**Table 4.** Distribution of sex predication in studied group.

Next, a correlation heatmap was plotted in order to visualize the strength of relationships between all measured dimensions (Fig. 8). These data revealed that HL had a strong positive correlation with EE’ and DD’ variables. Where those dimensions (EE’ and DD’) were actually participated in hyoid bone length (HL). Besides, there was a positive correlation between HW and DE’, and GG’ dimensions, which directly related to the width of hyoid bone. AA’ and FF’ were also strongly correlated to each other.

Pairwise comparisons represented in Fig. 9, summarize all data about the measured parameters of hyoid bone in males and females.

**Meta-analysis**

Next, the data obtained from the present study were contrasted with those from other 12 populations through a meta-analysis study. Those other 12 studies included Croatian<sup>23</sup>, American<sup>4</sup>, Japanese<sup>19</sup>, Italian<sup>13</sup>, Turkish<sup>24</sup>, Korean<sup>25</sup>, Indian<sup>26</sup>, European<sup>27</sup>, Anatolian<sup>28</sup>, French<sup>29</sup>, Saudi<sup>10</sup>, and Iranian<sup>30</sup> populations. The subgroups assessed were defined by the hyoid dimensions: major axis of hyoid bone<sup>4,13,19,24–27</sup>, the minor axis of hyoid bone<sup>4,10,13,19,23–29</sup> length of hyoid bone<sup>23,25–28,30</sup>, and distance between lesser horns<sup>10,19,23,26,28–30</sup>. The comparison of outcomes was between male and female values.

The heterogeneity amongst the subgroups varied from 42 to 94%. In order to compare the results, a random effects model with an inverse variance statistical approach was used. Due to the significant heterogeneity between the primary studies, a random effect model was applied in this metanalysis. A forest plot is typically deployed to illustrate the outcomes of a meta-analysis. The original articles’ contribution for each hyoid bone dimension, weighted mean difference, 95% confidence interval, heterogeneity test, and overall significance test of the measured parameters for each group are displayed in Fig. 10. Whereas the CIs of all individual studies don’t cross the line-of-no-effect, which denoting the difference in outcome statistically significant, except the minor axis of hyoid bone in Lekšan et al.<sup>23</sup> study and, the minor axis of hyoid bone, hyoid bone length and distance between lesser horns in Kopuz and Ortug<sup>28</sup> study. The CI of the pooled estimate entirely veers to the left of the line-of-no-effect indicating a substantial increase in measured hyoid dimensions ( $P < 0.00001$ ).

The comparison of studies on hyoid bones measurement between males and females showed a highly significant increase in major axis (mean 3.98 mm), minor axis (mean 1.53 mm), hyoid length (mean 5.28 mm), and distance between lesser horns (mean 3.83 mm). Moreover, Lekšan et al.<sup>23</sup> and Kopuz and Ortug<sup>28</sup> observed a substantial decrease in the minor axis (mean –0.40 mm), and in the length (mean –0.46 mm) of hyoid bone measurements, respectively, but they did not find any statistically worthy modulation in the overall effect.

As depicted in Fig. 10, a sub-analysis was performed for the major axis of hyoid bone between males and females, using random effects modeling for the 8 case series studies ( $n = 787$  males and 675 females) providing mean  $\pm$  SD, and the MD was 3.98 (95% CI 3.24, 4.73; overall effect  $Z = 10.46$ ;  $P < 0.00001$ ; Q statistic  $< 0.00001$ ;  $I^2 = 87\%$  with high inconsistency). Another sub-analysis was performed for the minor axis of hyoid bone between males and females, using random effects modeling for the 1<sup>2</sup> case series studies ( $n = 992$  males and 802 females) providing mean  $\pm$  SD, and the MD was 1.35 (95% CI 1.12, 1.57; overall effect  $Z = 11.56$ ;  $P < 0.00001$ ; Q statistic = 0.00;  $I^2 = 64\%$  with moderate inconsistency). However, that was performed for the length of hyoid bone between males and females, using random effects modeling for the 9 case series studies ( $n = 713$  males and 602 females) providing mean  $\pm$  SD, and the MD was 5.28 (95% CI 3.70, 6.86; overall effect  $Z = 6.55$ ;  $P < 0.00001$ ; Q statistic  $< 0.00001$ ;  $I^2 = 94\%$  with high inconsistency). Finally, the sub-analysis was performed between the distances of lesser horns in males and females, using random effects modeling for the 8 case series studies ( $n = 881$  male, 767 female) providing M  $\pm$  SD, and the MD was 3.83 (95% CI 3.47, 4.19; overall effect  $Z = 20.99$ ;  $P < 0.00001$ ; Q statistic = 0.10;  $I^2 = 42\%$  at low inconsistency). The following parameters had substantial weighted mean differences and significant heterogeneity: major axis (3.98 mm), minor axis (1.35 mm), and length of the hyoid bone (5.28 mm), which are graphically shown in Fig. 10. Significant weighted mean difference with insignificant heterogeneity was found for the distance between lesser horns (3.83 mm).

**Machine learning approach**

The application of machine learning algorithms to estimate sex based on hyoid bone measurements yielded promising results (Table 5; Fig. 11).

Before hyperparameter tuning, the models demonstrated varying levels of accuracy, precision, recall, and F1 score. Gradient Boosting, KNN, GNB, and SVM classifiers exhibited high accuracies ranging from 0.9 to 0.933. Logistic Regression and the Voting Classifier also achieved high accuracy scores of 0.933. However, Random Forest and Decision Tree classifiers showed slightly lower accuracy scores of 0.8334 to 0.9.

After hyperparameter tuning, the models generally showed improvements in their performance metrics. Notably, KNN achieved the highest accuracy of 0.933, with precision, recall, and F1-score also reaching 0.9.

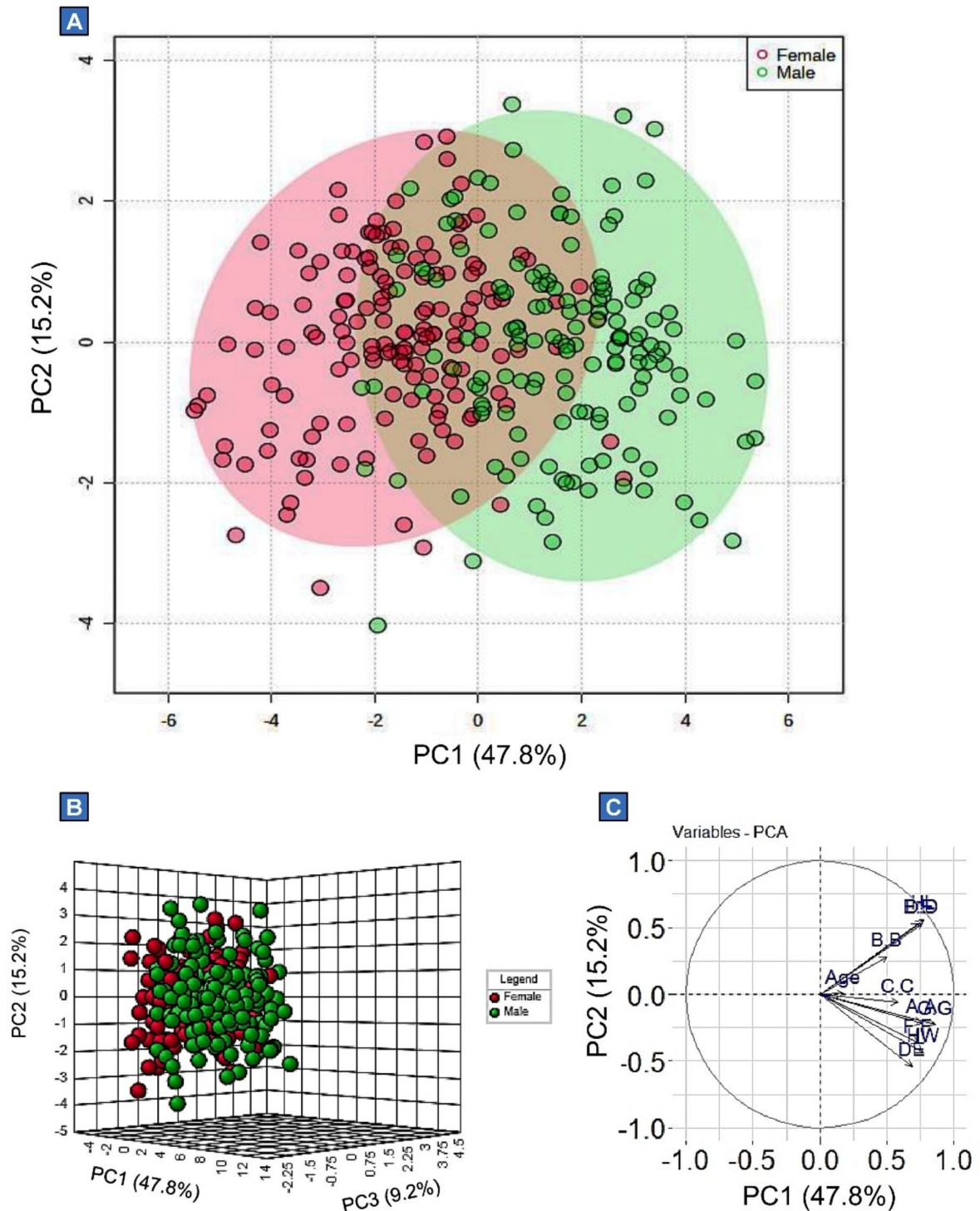


**Fig. 6.** Principal component analysis (PCA). (A) Biplot Score of PC1 and PC2 of all variables in male and female groups. (B) 3D PCA plot showing PC1, PC2, and PC3 of all variables in male and female groups. (C) PCA loading plot. PC principal component.

Logistic Regression and the Voting Classifier maintained their high accuracy scores of 0.933, with consistent precision, recall, and F1-score values of 0.9. Other models, including Gradient Boosting, Random Forest, Gaussian Naïve Bayes, and SVM, also demonstrated improved performance metrics, with accuracies ranging from 0.9 to 0.933.

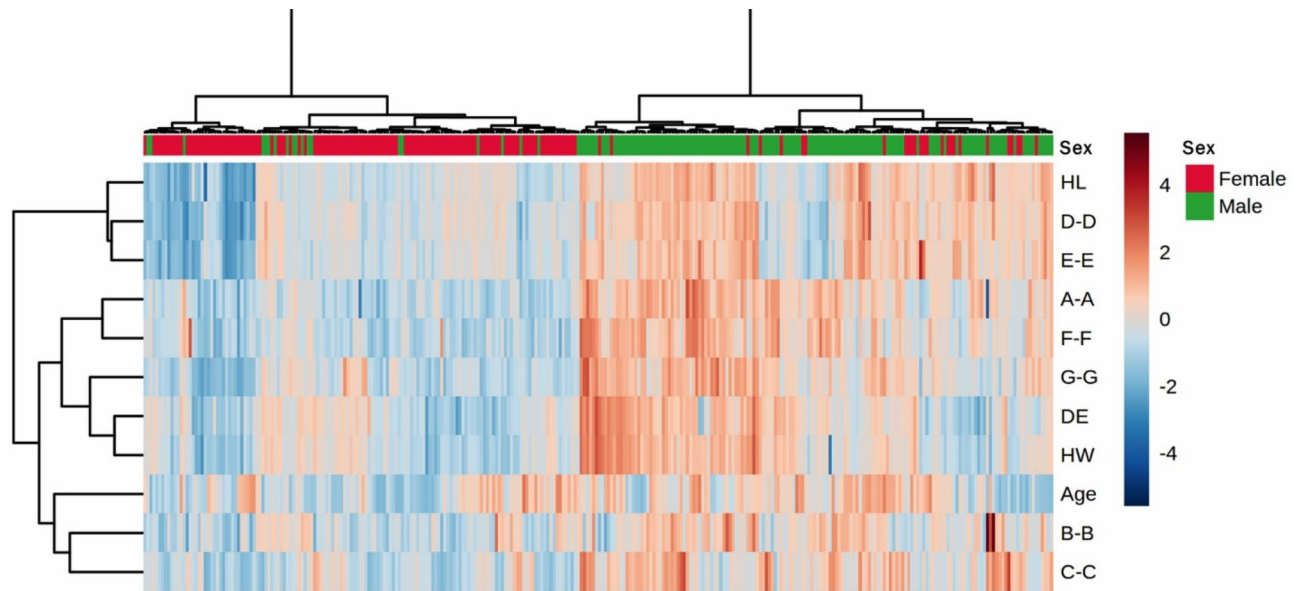


**Fig. 7.** Heatmap clustering of the measured dimensions of hyoid bone in males and females. Color bar indicates increased (red) and decreased (blue) length of the hyoid bones in males and females. A normalized Z score data matrix was used to generate a heatmap. Each colored cell on the map denotes the mean of measured dimensions in rows and male and female in columns. Dark red is the highest value on the gradation scale, and blue represents the lowest value.

Furthermore, the Voting Classifier, which combined predictions from multiple models, showed competitive performance with an accuracy of 0.933 and consistent precision, recall, and F1 score values of 0.9.

The variable importance plot of the Random Forest regression model in predicting sex is displayed in Fig. 12. Variable importance plot shows the relative importance of each variable as a predictor of sex. The important metric considered for analysis is the means of decrease in accuracy calculated using Random Forest Classification Algorithm. The top variables in importance for sex prediction were AA', BB', FF', and HL (mean decrease accuracy).

## Discussion

Sex is one of the most crucial aspects of identification. Sexual dimorphic traits of the hyoid bone, render it a credible option for determining an individual's sex from ambiguous skeletal remains<sup>12,31</sup>. The measurement utilizing 3D CT imaging is unpretentious and has great precision, and it can be used efficaciously in forensic medicine. 3D MDCT data can be gained without the impact of any artifact with the ability to erase the peripheral soft tissues so that the hyoid bone tissue alone is precisely visualized<sup>19</sup>.

Our results emphasize the hyoid bone sexual dimorphism, all 10 assessed measurements exhibited a statistically significant difference between males and females. Males' hyoid bone is longer in the anterior-posterior direction (longer HL) because greater horns are noticeably longer, and they are broader, as evidenced by longer distances between greater horns while females have shorter horns and narrower hyoid bone. Overall, according to our observations, the hyoid bone dimensions of males were considerably larger than those of females. A possible explanation for this is the stature disparities may account for the sexual dimorphism of hyoid bone measures<sup>2,30</sup>. We postulated that to androgen signaling which is crucial for this sexual dimorphism<sup>32</sup>. In men, increases in testosterone promote substantial gains in muscle mass, coinciding with significant growth in bone dimensions and sturdiness<sup>33</sup>. Overwhelming evidence was in endorsement with our result that males' hyoid bone metric values were noticeably greater than those of females<sup>4,9,19,24,25,27,31,34,35</sup>. Additionally, incongruent with that obtained by<sup>30,36,37</sup>, who found that males have a greater hyoid bone width as compared to females. Furthermore, the present study concurs with the previous literature released by Lekšan et al.<sup>23</sup> and Okasi et al.<sup>12</sup> who claimed that male hyoid bone length was greater than that of female counterpart. Besides, those who reported a longer length and larger hyoid body in males compared to females<sup>9,31</sup>.

It has been reported that sexual dimorphism patterns differ among populations, and the functions gained could not have the same level of precision if applied to other populations<sup>14</sup>. Although numerous hyoid bone metric sex predictors have been identified, however, due to racial differences, they are often helpful only for the populations under study. The present data indicated that all dimensions exhibited significant differences among sex ( $P < 0.01$ ), therefore, they could be utilized to estimate the sex by employing discriminant function equations. In the current univariate discriminant analysis, AA' exhibited the greatest percentage of accuracy (85%) in sex estimation confirming the data obtained from the PCA. Congeners to the former studies the maximum degree of

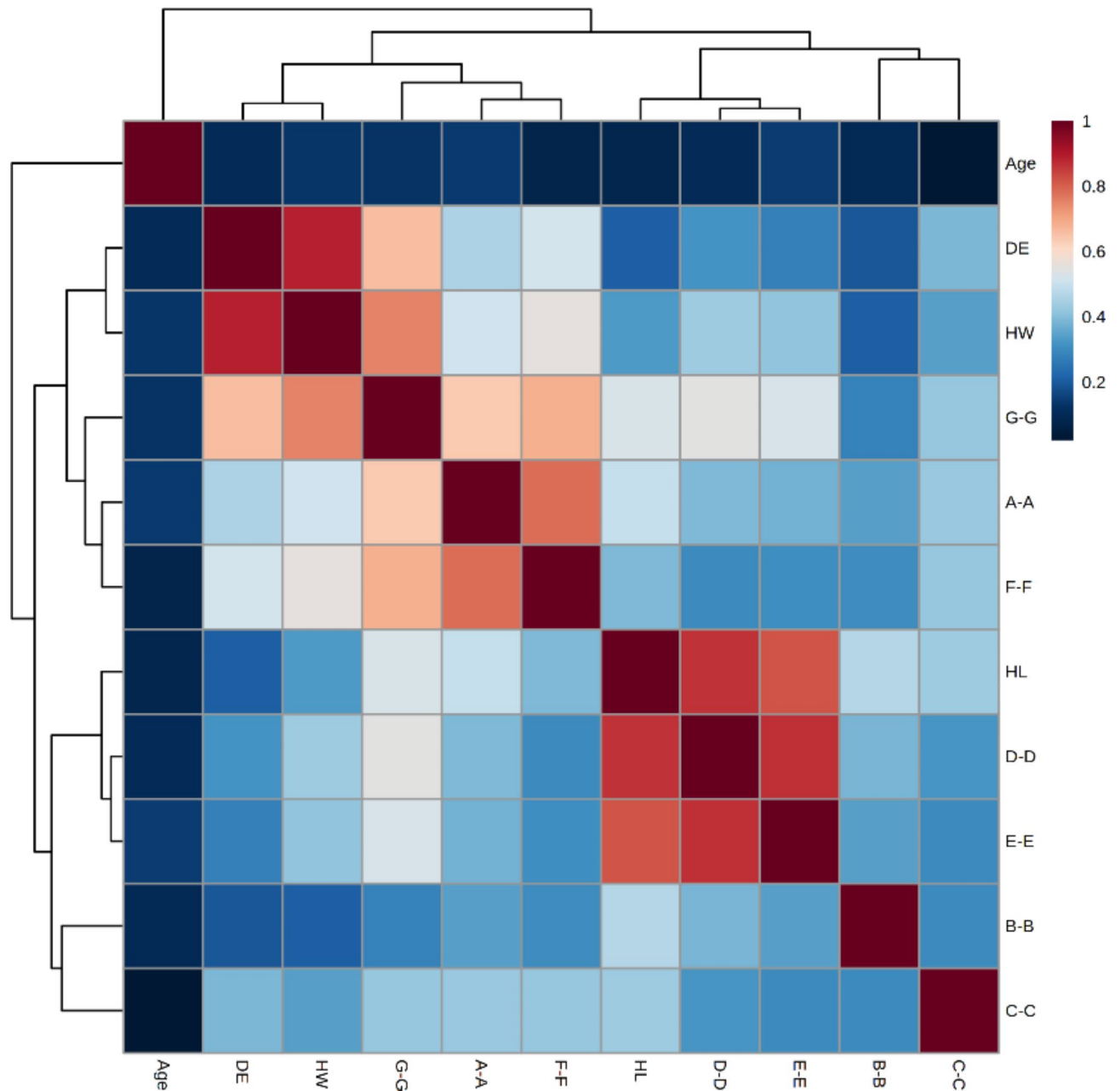


**Fig. 8.** Correlation heatmap of all tested variables in hyoid bone. The color-coding of the cells indicates the strength and type of relationship among variables. Red or blue-colored cells indicate the existence of positive or negative correlations, respectively. Color intensity determines the strength of the correlation.

sexual dimorphism was provided by the linear distance between the most lateral edges of the hyoid body, which displayed the highest level of sexual dimorphism with a success rate  $> 80\%$  in sex prediction<sup>2,6,27</sup>. D'Anastasio et al.<sup>13</sup> reported that univariate analysis applying the maximum length of the hyoid body in the transverse plane yielded an 80% accuracy rate. Allocation accuracy of these functions ranged from 60.7 to 80% in males and 66–90% in females. Hence, discriminant functions tend to classify females more precisely than males. Allocation accuracy for both sexes pooled ranges from 65.7 to 85%. Considering these findings, sex can be identified even if there is no other bone is available except the hyoid body, especially when fragmented or incomplete hyoid bones found in skeletal remains<sup>2,13</sup>. In reality, when sex determination of a decayed body or a partially skeletonized corpse is required, the hyoid bone joints are often damaged by taphonomic phenomena<sup>2</sup>.

Stepwise discriminant analysis, based on a combination of the four measurements (AA', BB', FF', and HL) yielded increased accuracy rates for sex estimation than univariate functions. This result confirming the data obtained from loading plot PCA. Overall, 87.7% of the dataset was properly categorized by this model into their groups. The accuracy for women was higher (90%) than for men (85.3%) at the individual group level. This high accuracy reveals that metric assessment of hyoid bone can be a valuable and precise tool for sex identification



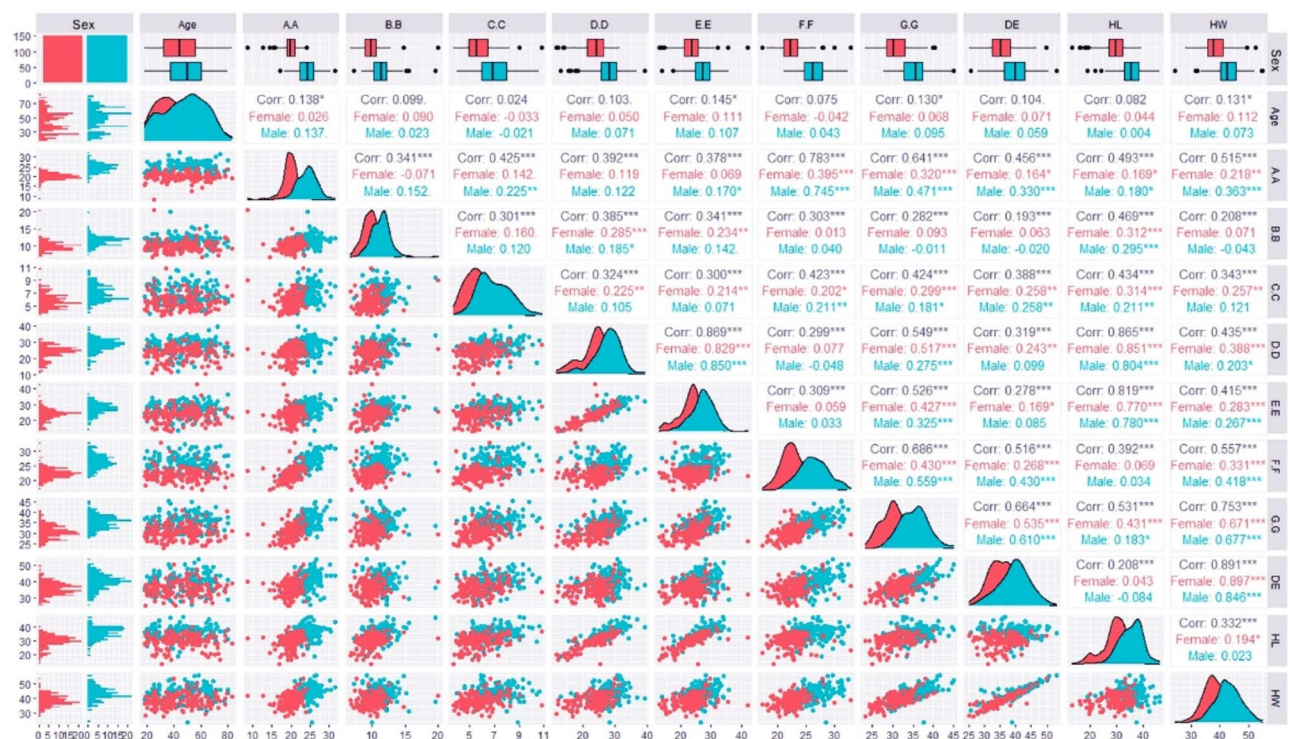


**Fig. 9.** Pairwise comparisons of the measured dimensions of hyoid bone in males and females. Blue and red color indicate male and female, respectively.

of Egyptian skeletal relics and can foretell even in cases when the hyoid bone is the only bone present<sup>6</sup>. Also, 90% of the cases were correctly classified by this four-variable model, according to cross-validated data. A number of studies have shown that a combination of multiple measurements of the hyoid bones gives better accuracies of more than 90% for sex determination in various populations<sup>2,4</sup>. A 90% accuracy of sex prediction was achieved in the study of Mukhopadhyay<sup>38</sup> on Indians utilizing a combination of five metrics (including our 3 measurements FF, AA, and HL). A study done by Soltani et al.<sup>30</sup> on Iranians, found a combination of distance between the lesser horns (distance B) and the length of hyoid bone (distance C) as predictors of sex yielded an increased accuracy of 97.4% for sex categorization. In Kindschuh et al.<sup>39</sup> study, on Americans, the width of the, and total hyoid length, showed significant sex differences. In a study done by Kim et al.<sup>25</sup> on 85 corpses in Korea, established an equation that comprised 3 linear measurements and achieved 88.2% accuracy for sex identification; although one of them was BL and the two other measurements were different from ours. In another study in Turkey, conducted on adult cadavers, three hyoid measurements (one of them, hyoid bone length, included in our equation) were utilized and the data revealed 77.4% classification accuracy for males and 81.3% for females<sup>24</sup>. These findings imply that when hyoid bone is intact, sex can be predicted with high precision and great confidence. Sex estimation in our study using the combination of best metric predictors does not guarantee better sex prediction accuracy in females while the accuracy increased in males than in univariate discriminate analysis.

The comparisons used in our meta-analysis were done in hyoid bone dimensions between males and females. Through 13 studies, the meta-analysis revealed a significant increase in every dimension analyzed, except Lekšan et al.<sup>23</sup> and Kopuz and Ortug<sup>28</sup> found decreases in the minor axis of hyoid bone and hyoid bone length, respectively, but without significant changes in the overall effect. The current meta-analysis also detected a significant difference between studies. Considering the available information, there is strong evidence to deduce that the major axis, minor axis, hyoid bone length, and distance between lesser horns dimensions can help to differentiate between males and females among populations.

Contrary to traditional classification approaches, machine learning algorithms enable the classification of non-linear relationships between predictor and outcome variables with generally better classification accuracies<sup>16</sup>. Although many studies use both approaches independently, to the best of our knowledge, there is limited literature on using both discriminant analysis and machine learning to predict sex types based on the hyoid bone. The current study is unique as it incorporates machine learning techniques for accurate sex detection after using traditional discriminant analysis as a PCA to identify the best predictor variables. Our machine learning models indicate effective utilization of hyoid bone measurements to predict sex, with accuracies ranging from 0.8667 to 0.933 after hyperparameter tuning. Similarly to the current study, mutlu et al.<sup>40</sup> found that 95.4% accuracy was achieved using an artificial neural network, compared to 92.9%, which was the maximum sex estimation accuracy that was obtained with DFA. The current data demonstrate how machine learning and discriminant analysis may be used in conjunction to predict biological sex using hyoid bones. The

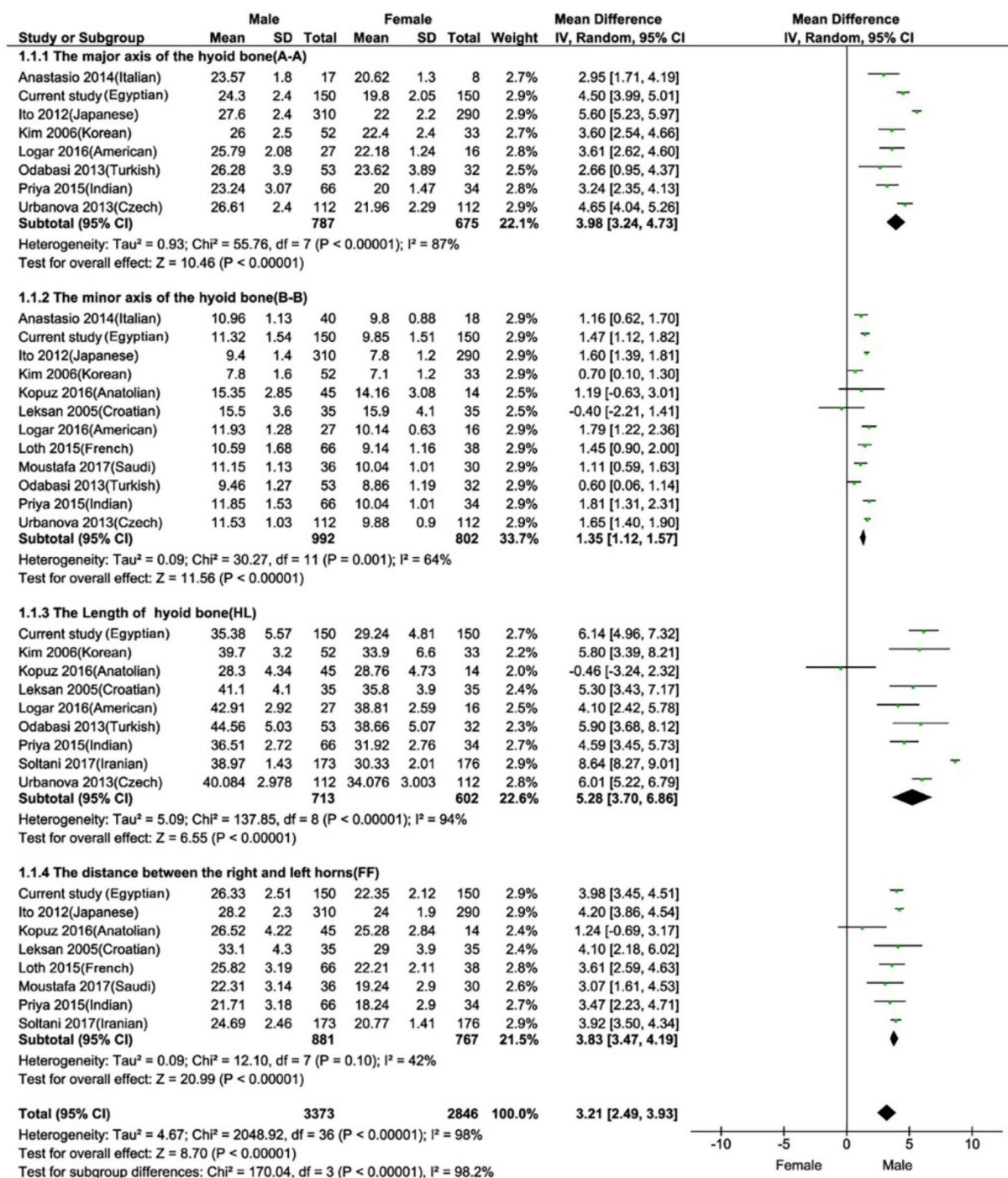


**Fig. 10.** Forest plot of male and female mean difference for hyoid bone measurements. The line-of-no-effect (vertical line) separates outcomes that favor males and females. The squared green boxes represent the point of the estimate, and the horizontal lines represent the associated 95% confidence intervals for each study.  $\chi^2$  chi-square,  $CI$  confidence interval,  $df$  degree of freedom,  $IV$  independent variable,  $SD$  standard deviation,  $\tau^2$  tau-square.

robust performance of these models underscores the utility of machine learning approaches in complementing traditional statistical methods for forensic sex determination based on skeletal remains.

Model	Tunning hyperparameters							
	Accuracy		Precision		Recall		F1-score	
	Before	After	Before	After	Before	After	Before	After
Gradient boosting	0.9	0.9	0.889	0.889	0.8	0.8	0.8421	0.8421
Random forest	0.8334	0.9	0.7	0.889	0.7	0.8	0.7	0.842
KNN	0.9	0.933	0.8889	0.9	0.8	0.9	0.842	0.9
GNB	0.9	0.9	0.8889	0.8889	0.8	0.8	0.842	0.842
SVM	0.9	0.9	0.889	0.889	0.8	0.8	0.842	0.842
Decision tree classifier	0.8334	0.8667	0.8571	0.875	0.6	0.7	0.7059	0.7778
Logistic regression	0.933	0.933	0.9	0.9	0.9	0.9	0.9	0.9
Voting classifier	0.8667	0.9333	0.875	0.9	0.7	0.9	0.7778	0.9

**Table 5.** The performance metrics of each model before and after hyperparameter tuning. *GNB* Gaussian Naïve Bayes, *KNN* K-nearest neighbors, *SVM* support vector machine.

Conclusion

Based on our study findings, males had larger hyoid bone than females as all measured hyoid bone dimensions are statistically greater in males than females. The discriminant equation developed in this study from hyoid bone applies to the Egyptian population, however, may not apply to non-Egyptian populations. In addition, 3D MDCT is an effective and reliable tool for hyoid bone measurements. The combination of hyoid bone length, the distance between the lesser horns, the major axis, and the minor axis of hyoid bones are the most accurate dimensions helping proper and accurate sex discrimination. While hyoid body width displayed the highest accuracy rate (85%) and most significantly contributed to sex determination in the case of fragmented or incomplete hyoid bones. Furthermore, applying machine learning methods and image processing techniques can offer a further advantage in sex prediction. Hyoid bone is an extremely sexually dimorphic bone in contemporary Egyptians as well and may help the forensic interrogator for sex discrimination with a higher level of accuracy. The results of this research will motivate future researchers to use machine learning techniques to examine various bone data and enhance the functionality of machine learning models.



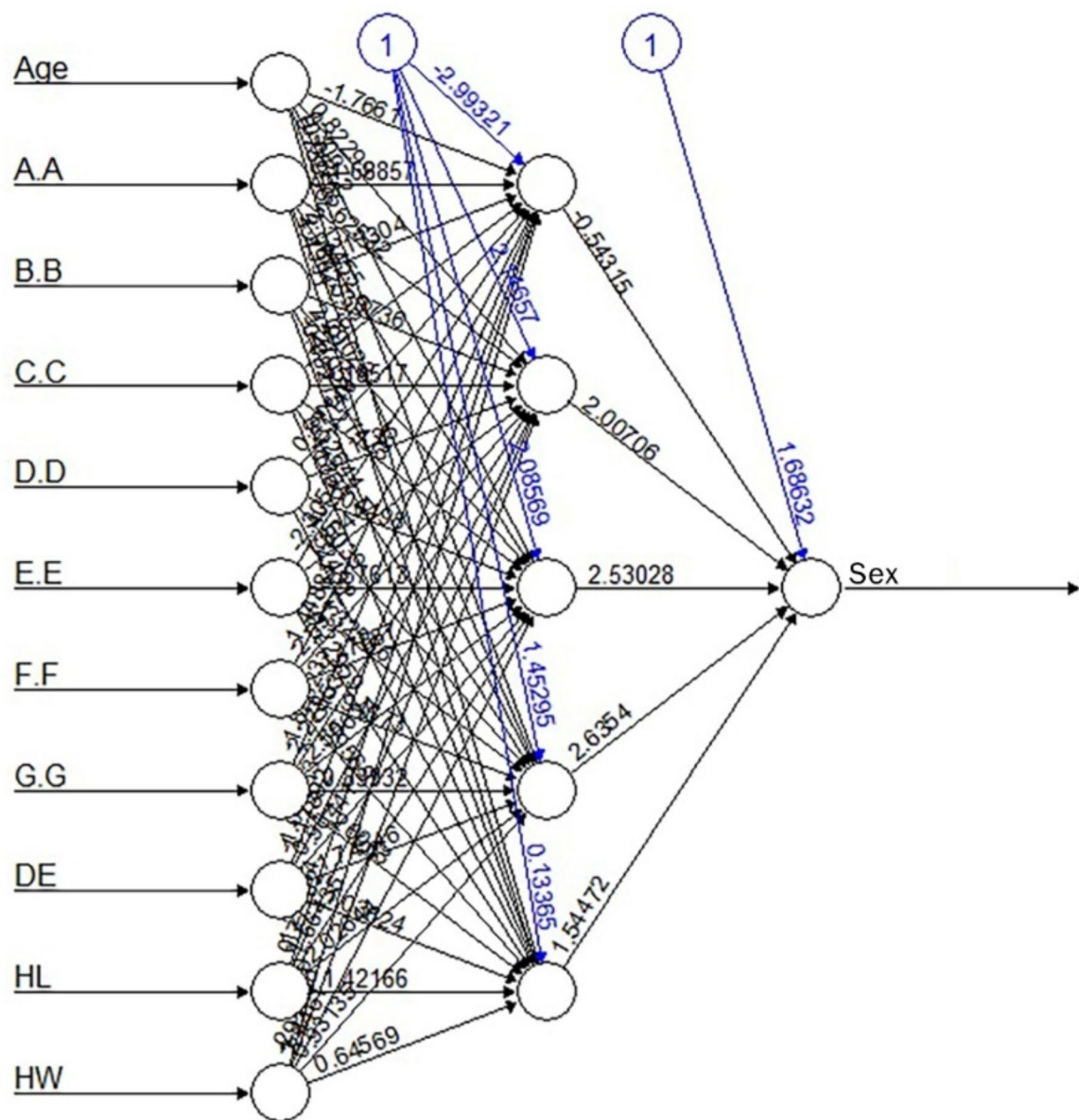


**Fig. 11.** Visual representations of ANNs algorithm for sex prediction of hyoid bone parameters. ANNs artificial neural networks.

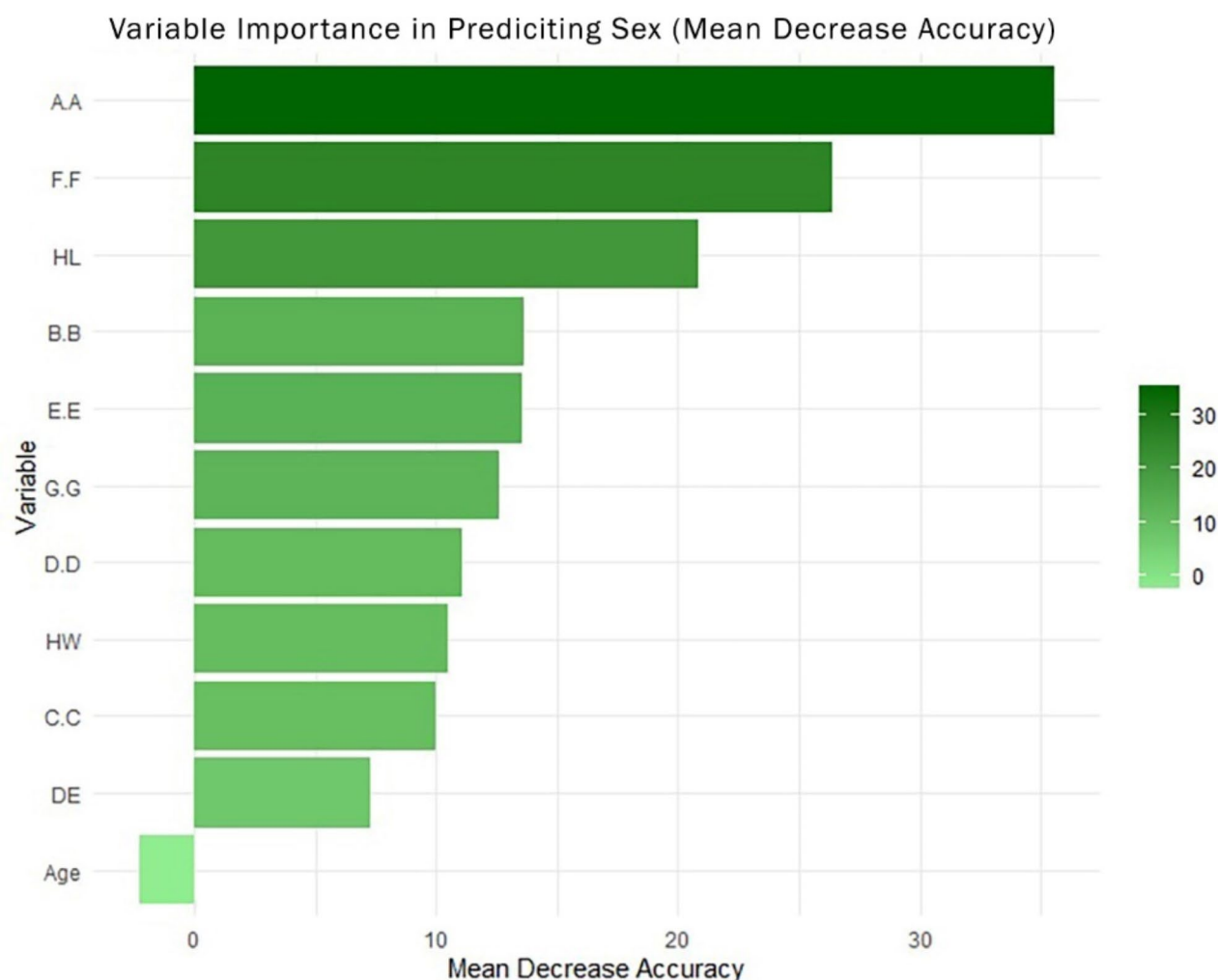


**Fig. 12.** Variable importance plot of Random Forest model in predicting sex. The variables are presented in descending importance. The higher the value of mean decrease accuracy, the higher the importance of the variable in the model.

### Data availability

The datasets used and analyzed during the current study are available from the corresponding author upon request.

Received: 11 July 2024; Accepted: 3 January 2025

Published online: 21 January 2025

### References

1. Elmadawy, M. A. et al. Telomere length and signal joint T-cell receptor rearrangement excision circles as biomarkers for chronological age estimation. *Biomarkers* **26**, 168–173 (2021).
2. Torimitsu, S. et al. Determination of sex on the basis of hyoid bone measurements in a Japanese population using multidetector computed tomography. *Int. J. Leg. Med.* **132**, 907–914 (2018).
3. Özer, I., Katayama, K., Sağır, M. & Güleç, E. Sex determination using the scapula in medieval skeletons from east Anatolia. *Coll. Antropol.* **30**, 415–419 (2006).
4. Logar, C. J., Peckmann, T. R., Meek, S. & Walls, S. G. Determination of sex from the hyoid bone in a contemporary White population. *J. Forensic Leg. Med.* **39**, 34–41 (2016).
5. Lucas, V. S., McDonald, E., Andiappan, M. & Roberts, G. Dental age estimation—Root pulp visibility (RPV) patterns: A reliable mandibular maturity marker at the 18 year threshold. *Forensic Sci. Int.* **270**, 98–102 (2017).
6. Köse, E. & Bulut, D. G. The use of hyoid bone dimensions in age and sex estimation in a Turkish population: A cone-beam computed tomography study. *Folia Morphol.* **81**, 183–189 (2022).
7. AlJulaih, G. H. & Menezes, R. G. Anatomy, head and neck, hyoid bone. *StatPearls* at <http://www.ncbi.nlm.nih.gov/pubmed/30969548> (2019).
8. Kumar, T. & Rudra, A. Estimation of various measurements of hyoid bone and its co-relation with sex of the individual—An autopsy study. *J. Med. Sci. Clin. Res.* **6**, 644–652 (2018).



9. Fakhry, N. et al. Analysis of hyoid bone using 3D geometric morphometrics: An anatomical study and discussion of potential clinical implications. *Dysphagia* **28**, 435–445 (2013).
10. Moustafa, S. Estimation of sex from hyoid bone: A preliminary study with medico-legal implications. *Ain Shams J. Forensic Med. Clin. Toxicol.* **29**, 1–6 (2017).
11. Gnanadev, R., Iwanaga, J., Loukas, M. & Tubbs, R. S. An unusual finding of the hyoid bone. *Cureus* <https://doi.org/10.7759/cureus.3365> (2018).
12. Okasi, A., Sadeghian, M. H., Behnouth, B. & Rad, A. S. Sex identification by morphometric study of hyoid bone. *Int. J. Med. Toxicol. Forensic Med.* **8**, 145–150 (2018).
13. D'Anastasio, R. et al. Estimation of sex from the hyoid body in skeletal individuals from archeological sites. *HOMO J. Comp. Hum. Biol.* **65**, 311–321 (2014).
14. Abdelaleem, S., Hassan, O., Abdelazeem, I. & Abdelkader, M. Role of patellar imaging using 3D computed tomography in determination of sex and stature in upper Egypt population. *Int. J. Forensic Sci. Pathol.* **4**, 289–296 (2016).
15. Tyagi, A., Tiwari, P., Bhardwaj, P. & Chawla, H. Prognosis of sexual dimorphism with unfused hyoid bone: Artificial intelligence informed decision making with discriminant analysis. *Sci. Justice* **61**, 789–796 (2021).
16. Kartal, E. et al. Sex estimation using foramen magnum measurements, discriminant analyses and artificial neural networks on an eastern Turkish population sample. *Leg. Med.* **59**, 102143 (2022).
17. Nikita, E. & Nikitas, P. On the use of machine learning algorithms in forensic anthropology. *Leg. Med.* **27**, 101771 (2020).
18. Amin, M. F. & Hassan, E. I. Sex identification in Egyptian population using multidetector computed tomography of the maxillary sinus. *J. Forensic Leg. Med.* **19**, 65–69 (2012).
19. Ito, K. et al. Morphological study of the human hyoid bone with three-dimensional CT images—Gender difference and age-related changes. *Okajimas Folia Anat. Jpn.* **89**, 83–92 (2012).
20. Salem, N. H. et al. Age estimation and sex determination by CT-scan analysis of the hyoid bone—Application on a Tunisian population. *La Rev. Méd. Lég.* **11**, 137–144 (2020).
21. Higgins, J. P. T., Thompson, S. G., Deeks, J. J. & Altman, D. G. Measuring inconsistency in meta-analyses. *BMJ* <https://doi.org/10.1136/bmj.327.7414.557> (2003).
22. Attia, A. H. & Said, A. M. Brain seizures detection using machine learning classifiers based on electroencephalography signals: A comparative study. *Indones. J. Electr. Eng. Comput. Sci.* **27**, 803–810 (2022).
23. Lekšan, I., Marcikić, M., Nikolić, V., Radić, R. & Selthofer, R. Morphological classification and sexual dimorphism of hyoid bone: New approach. *Coll. Antropol.* **29**, 237–242 (2005).
24. Balseven-Odabasi, A. et al. Age and sex estimation by metric measurements and fusion of hyoid bone in a Turkish population. *J. Forensic Leg. Med.* **20**, 496–501 (2013).
25. Kim, D.-I. et al. Morphometrics of the hyoid bone for human sex determination from digital photographs. *J. Forensic Sci.* **51**, 979–984 (2006).
26. Priya, K. D. V. S. & Ranzeetha, D. Determination of sex from morphometry of hyoid bone. *Indian J. Clin. Anat. Physiol.* **2**, 157 (2015).
27. Urbanová, P., Hejna, P., Zátoková, L. & Šafr, M. What is the appropriate approach in sex determination of hyoid bones?. *J. Forensic Leg. Med.* **20**, 996–1003 (2013).
28. Kopuz, C. & Ortug, G. Variable morphology of the hyoid bone in anatolian population: Clinical implications—A cadaveric study. *Int. J. Morphol.* **34**, 1396–1403 (2016).
29. Loth, A. et al. Analysis of hyoid-larynx complex using 3D geometric morphometrics. *Dysphagia* **30**, 357–364 (2015).
30. Soltani, S., Aghakhani, K. & Fallah, F. Sex prediction potential of hyoid metric measurements in Iranian adults. *Leg. Med.* **25**, 6–10 (2017).
31. Werner, H. M., Miller, C. A., Tillman, K. K., Wang, Y. & Vorperian, H. K. Growth and sexual dimorphism of the hyoid bone and its relationship to the mandible from birth to 19 years: A three-dimensional computed tomography study. *Anat. Rec.* **304**, 1901–1917 (2021).
32. Laurent, M. et al. Androgens and estrogens in skeletal sexual dimorphism. *Asian J. Androl.* **16**, 213–222. <https://doi.org/10.4103/1008-682X.122356> (2014).
33. Lang, T. F. The bone-muscle relationship in men and women. *J. Osteoporos.* **2011**, 1–4. <https://doi.org/10.4061/2011/702735> (2011).
34. Mukhopadhyay, P. P. Morphometric features and sexual dimorphism of adult hyoid bone: A population specific study with forensic implications. *J. Forensic Leg. Med.* **17**, 321–324 (2010).
35. Sameera, S. S. & Rao, K. E. V. Morphometric analysis and sexual dimorphism of hyoid bone in Telangana population. *Int. J. Anat. Res.* **7**, 7038–7041 (2019).
36. Shangase, M. O., Ishwarkumar, S., Pillay, P. & Morphology, P. Morphology and morphometry of the hyoid bone in a black South African population. *Int. J. Morphol.* **39**, 134–137 (2021).
37. Vohra, P. & Kulkarni, P. Sexual dimorphism of human hyoid bone. *Int. J. Anat. Res.* **5**, 3607–3610 (2017).
38. Mukhopadhyay, P. P. Determination of sex from an autopsy sample of adult hyoid bones. *Med. Sci. Law* **52**, 152–155 (2012).
39. Kindschuh, S. C., Dupras, T. L. & Cowgill, L. W. Determination of sex from the hyoid bone. *Am. J. Phys. Anthropol.* **143**, 279–284 (2010).
40. Mutlu, G. D. et al. Sex estimation from the hyoid bone measurements in an adult Eastern Turkish population using 3D CT images, discriminant function analysis, support vector machines, and artificial neural networks. *Leg. Med.* **67**, 102383 (2024).

## Acknowledgements

The authors thank all supports offered by Princess Nourah bint Abdulrahman University Researchers Supporting Project number (PNURSP2025R127), Princess Nourah bint Abdulrahman University, Riyadh, Saudi Arabia. This work is also supported via funding from Prince Sattam bin Abulaziz University project number (PSAU/2024/R/1446) and Researchers Supporting Project number (MHIRSP2024009), AlMaarefa University, Riyadh, Saudi Arabia. The deanship of Scientific Research at Northern Border University, Arar, KSA, funded this research work through the project number "NBU-FFR-2025–2510-02. Moreover, this research is partially funded by Zarqa University-Jordan. This paper is also published from the own research funds of the University of Life Sciences "King Mihai I" from Timisoara, Romania. We also appreciate the help of Eng. Mazen M. Yassin, teaching assistant at the Minia University Faculty of Engineering's Biomedical Engineering Department, in implementing the AI data.

## Author contributions

Conceptualization, A. Abdelkader and A. Abdeen. Data curation, A. Abdelkader, S.A.A., A.Y.A.H., M.A., A.M.S., D. A., A. M. A., K. A. B., and A. Abdeen. Formal analysis, A. Abdelkader, S. A. A., E.E., M. A., A.M.S. and A. Abdeen. Supervision, A. Abdelkader and A. Abdeen. Methodology, A. Abdelkader, A. Y. A. H, S. A. A, A.Y.

(A) H, (B) D. I., and A. M. A. Validation, A. Abdelkader, S. A. A, D. A., M.E., L. F, T. H., and E.S.T. Visualization, A. Abdeen, S.F.I., T.H., E.S.T., E.M.E., and A.M.S. Software, A. Y. A. H., M.E., S.F.I., and E.M.E. Resources, A. Abdelkader, E.S.T., M.E., E.E.E., S.F.I., and A. Abdeen. Writing—original draft, all authors Writing—review and editing, A. Abdelkader, A. Abdeen, E.S.T, T. H., E. M. E., K. A. (B), and M. O. All authors read and approved the final manuscript.

## Declarations

## Competing interests

The authors declare no competing interests.

## Ethics and consent to participate declarations

All participants agreed to participate.

## Ethical endorsement

The study was carried out in conformity with the guidelines of the International Council on Harmonization (ICH) and Islamic Organization for Medical Sciences (IOMS), the United States Office for Human Research Protections, and the United States Code of Federal Regulations and operates under Federal Wide Assurance N. FWA 000017585. The study protocol was also authorized by the Research Ethics Committee at the Faculty of Medicine, Ain Shams University, Egypt (Approval No. FMASU R09/2019).

## Additional information

**Correspondence** and requests for materials should be addressed to A.A., A.A. or B.-D.I.

**Reprints and permissions information** is available at [www.nature.com/reprints](http://www.nature.com/reprints).

**Publisher's note** Springer Nature remains neutral with regard to jurisdictional claims in published maps and institutional affiliations.

**Open Access** This article is licensed under a Creative Commons Attribution-NonCommercial-NoDerivatives 4.0 International License, which permits any non-commercial use, sharing, distribution and reproduction in any medium or format, as long as you give appropriate credit to the original author(s) and the source, provide a link to the Creative Commons licence, and indicate if you modified the licensed material. You do not have permission under this licence to share adapted material derived from this article or parts of it. The images or other third party material in this article are included in the article's Creative Commons licence, unless indicated otherwise in a credit line to the material. If material is not included in the article's Creative Commons licence and your intended use is not permitted by statutory regulation or exceeds the permitted use, you will need to obtain permission directly from the copyright holder. To view a copy of this licence, visit <http://creativecommons.org/licenses/by-nc-nd/4.0/>.

© The Author(s) 2025